Virus Research 370 (2026) 199761

Contents lists available at ScienceDirect

Virus Research

journal homepage: www.elsevier.com/locate/virusres

Toward *in planta* studies of persistent fungal viruses in a model plant

Paul Telengech [a,1], Sakae Hisano [a], Francesco Favaretto [a,b,c], Hiroaki Ichikawa [a,d], Kazuyuki Maruyama [a], Kiwamu Hyodo [a], Hideki Kondo [a], Nobuhiro Suzuki [a,d,*]

[a] Agrivirology Laboratory, Institute of Plant Science and Resources, Okayama University, Kurashiki, Okayama 710-0046, Japan
[b] Council for Agricultural Research and Economics - Research Centre for Viticulture and Enology (CREA-VE). Via XXVIII Aprile, 26, 31015 Conegliano TV, Italy
[c] University of Padua, Department of Agronomy, Food, Natural Resources, Animals and Environment, Agripolis, Viale dell'Università 16, 35020 Legnaro Pd, Italy
[d] Neo-Virology Laboratory, Graduate School of Agricultural Science, Tohoku University, Aoba 468-1, Sendai, Miyagi 980-8572, Japan

ARTICLE INFO

Keywords:
Cross-kingdom infection
Tissue culture
Partitivirus
dsRNA virus
Nicotiana, benthamiana
Callus
Suspension culture
Model plant

ABSTRACT

A model plant, *Nicotiana benthamiana*, was examined as a host for persistent fungal viruses capable of crossing organismal kingdoms. Protoplasts of *N. benthamiana* were transfected with a mixture of virions of a betapartitivirus, Rosellinia necatrix partitivirus 18 (RnPV18), and an alphapartitivirus, RnPV19, and were then subjected to plantlet regeneration. Primary RT-PCR-based screening showed that nearly 100% of the resulting calli tested positive for RnPV18, whereas approximately 90% were positive for RnPV19. However, secondary screening performed at a later stage of tissue culture revealed that only 6% of the calli retained RnPV19, whereas approximately 33% retained RnPV18. These results suggest that the calli were chimeric, consisting of virus-infected and virus-free sectors, and that the partitiviruses were progressively lost during callus maintenance. It is also possible that these fungal partitiviruses were unable to fully adapt to, or counteract, host defense responses sufficiently to establish stable infection. We succeeded in obtaining RnPV18-positive calli and suspension cultures that maintained the virus at detectable levels, as shown by northern blotting, after prolonged subculture for at least 9 months. High-throughput small RNA analyses revealed both similarities and differences in virus-derived small RNA profiles among protoplasts, calli, and suspension cultures. Viral genome analyses further revealed developmental stage-specific and stage-independent substitutions compared with the RnPV18 genomic sequence maintained in the original fungal host. Interestingly, a C-to-U mutation in the RNA-dependent RNA polymerase-encoding region of RnPV18 was detected much more frequently in a particular line, designated B21, than in another stably RnPV18-infected line, P8, irrespective of whether the virus was maintained in suspension cultures or calli. This may explain why virus accumulation in B21 calli and suspension cultures was much lower than that in P8 cell cultures, as RNA-seq analyses showed 159 K counts per million for P8 versus 44 K counts per million for B21. Taken together, this study provides a platform for investigating partitiviruses and other ubiquitous persistent viruses, which are generally difficult to inoculate experimentally.

1. Introduction

Fungal viruses generally establish asymptomatic infections, with some being efficiently transmitted to subsequent generations via spores (Ghabrial et al., 2015). Similarly, a group of plant viruses termed "persistent viruses" induce asymptomatic infections without visible macroscopic phenotypic alterations (Roossinck, 2010). These ubiquitous plant persistent viruses are characterized by extremely efficient vertical transmission through seeds (Roossinck, 2010). Although they are typically symptomless, they may occasionally exert physiological or ecological effects on their hosts, as exemplified by a plant mitovirus associated with enhanced tolerance to abiotic stress (Di Silvestre et al., 2022) and a plant endornavirus linked to cytoplasmic male sterility (CMS) in *Vicia faba* (Pfeiffer et al., 1993). However, due to

* Corresponding author at: Neovirology Laboratory, Innovation Center for Future Agricultural Production and Food Industry, Graduate School of Agricultural Science, 468-1 Aramaki Aza Aoba, Aoba-ku, Sendai, Miyagi 980-8572, Japan.
E-mail addresses: paultele05@gmail.com (P. Telengech), shisano@okayama-u.ac.jp (S. Hisano), francesco.favaretto@crea.gov.it (F. Favaretto), hiroaki.ichikawa.c7@tohoku.ac.jp (H. Ichikawa), k-maru@okayama-u.ac.jp (K. Maruyama), khyodo@okayama-u.ac.jp (K. Hyodo), hkondo@okayama-u.ac.jp (H. Kondo), nobuhiro.suzuki.e6@tohoku-u.ac.jp (N. Suzuki).
[1] Present address: Department of Plant Pathology, Kansas State University, 4024 Throckmorton PSC 1712 Claflin Road, Manhattan, KS 66506, USA.

https://doi.org/10.1016/j.virusres.2026.199761
Received 26 April 2026; Received in revised form 3 June 2026; Accepted 7 June 2026
Available online 7 June 2026

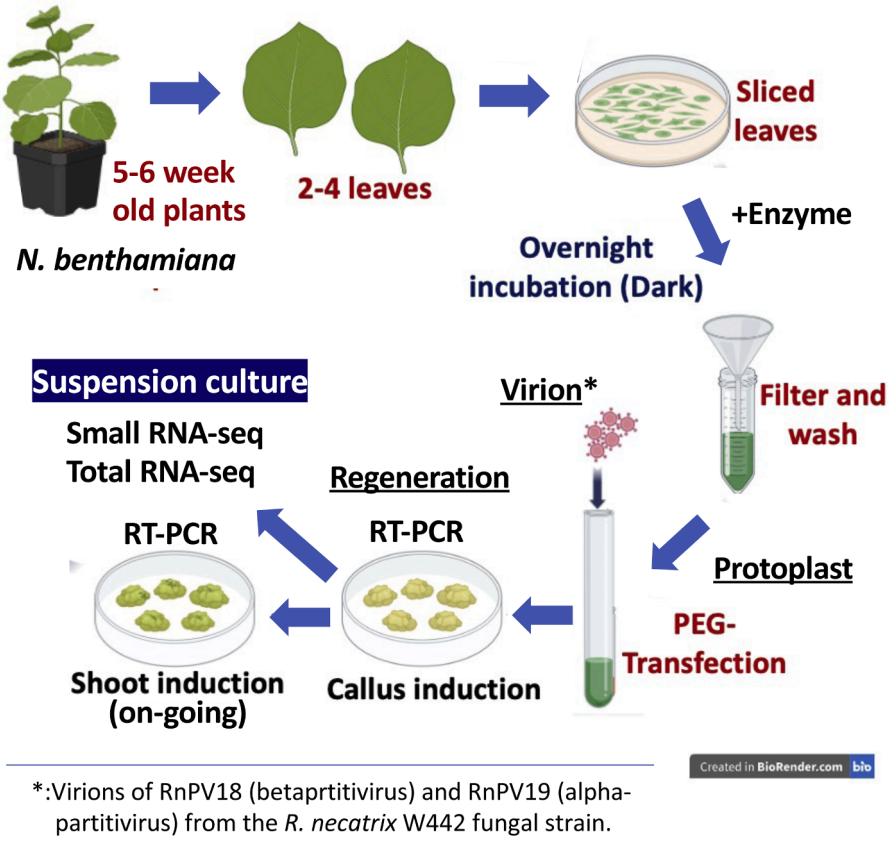

Fig. 1. Diagrammatic representation of virus transfection and regeneration of *Nicotiana benthamiana* protoplasts. Protoplasts were prepared from two to four young leaves by digesting cell wall. Virus particles of RnPV18 (a betapartitivirus) and RnPV19 (an alphapartitivirus) were co-purified from a single fungal (*Rosellinia necatrix*) strain, W442 and transfected into *N. benthamiana* protoplasts using the PEG method. The protoplasts were regenerated by culturing them first on callus induction media and then on shoot-inducing media. Mock-transfected protoplasts were cultured in parallel. See the Materials and Methods and Fig. 2 for details. The diagram was prepared with the help of BioRender.

the lack of reliable inoculation methods, it remains difficult to establish causal relationships between these viruses and host phenotypes. This contrasts with many fungal viruses, for which experimental inoculation systems are available (see below).

Interestingly, plant persistent viruses appear to share evolutionary origins with their counterparts infecting fungi and are often classified within the same genera as fungal viruses. These include encapsidated double-stranded RNA (dsRNA) viruses, such as cryptic viruses or partitivirids (Boccardo et al., 1987; Natsuaki et al., 1979; Vainio et al., 2018) and chrysovirids (Kotta-Loizou et al., 2020), as well as capsidless positive sense RNA viruses such as narnavirids (Esteban and Fujimura, 2021), mitovirids (Hillman and Cohen, 2021), and endornavirids (Valverde et al., 2019). In contrast to plant persistent viruses, many encapsidated fungal dsRNA viruses, and some capsidless positive-sense RNA viruses, can be experimentally introduced into new hosts via virion transfection (e.g., Sasaki et al., 2006; Shahi et al., 2021) or infectious cDNA transformation (Esteban and Fujimura, 2003). The existence of virus families and genera encompassing both plant and fungal viruses suggests that viruses may have moved, or may still move, between these two kingdoms (Plantae and Fungi). Indeed, trans-kingdom replication has been demonstrated for certain encapsidated dsRNA viruses, such as partitiviruses and totiviruses, between fungi and plants (Nerva et al., 2017; Telengech et al., 2024), as well as for single-stranded RNA viruses between plants and fungi, or between plants and insects (Bian et al., 2020; Dai et al., 2024).

Plant cell and tissue culture historically attracted considerable attention for both basic research and practical applications in plant breeding (Gelvin, 2003; Thorpe, 2012; Uchimiya and Murashige, 1974), and have recently regained importance in the era of genome editing technologies (Reed and Bargmann, 2021; Sukegawa et al., 2021; Yue et al., 2021). In virology, tobacco tissue culture was used as early as the 1960s and 1970s to establish synchronized replication systems for tobacco mosaic virus (Aoki and Takebe, 1969; Coutts et al., 1972; Takebe and Otsuki, 1969). More recently, we developed a method for establishing persistent systemic infection of carrot plants with fungal partitiviruses (Telengech et al., 2024), in which protoplasts were transfected with purified virus particles and regenerated into plants using tissue culture techniques.

Model plants such as *Arabidopsis thaliana* and *Nicotiana benthamiana* (Bombarely et al., 2012; Goodin et al., 2008; Meinke et al., 1998; Van Norman and Benfey, 2009) have been more extensively used than carrot for studying virus–host and virus–virus interactions. Efficient tissue culture systems enabling regeneration from protoplasts are well established for these species and are widely used in plant biology (Lin et al., 2018; Reed and Bargmann, 2021; Wu et al., 2023). We have therefore extended our previous carrot–partitivirus system to other host–virus combinations, particularly those involving the model plants *A. thaliana* and *N. benthamiana* (Bombarely et al., 2012; Garcia-Ruiz, 2019; Goodin et al., 2008; Ouibrahim and Caranta, 2013). The viruses used in these system are partitiviruses characterized by $T = 1$ capsids comprising 60 capsid protein (CP) homodimers and one or two RNA-dependent RNA polymerase (RdRP) molecules (Nibert et al., 2014). These systems offer a wide range of molecular tools, including mutant lines with impaired antiviral RNA silencing and well-characterized inoculable viruses (Andika et al., 2015; Brosseau and Moffett, 2015).

In this study, we report protocols for the inoculation of *N. benthamiana* with purified particles of fungal partitiviruses and

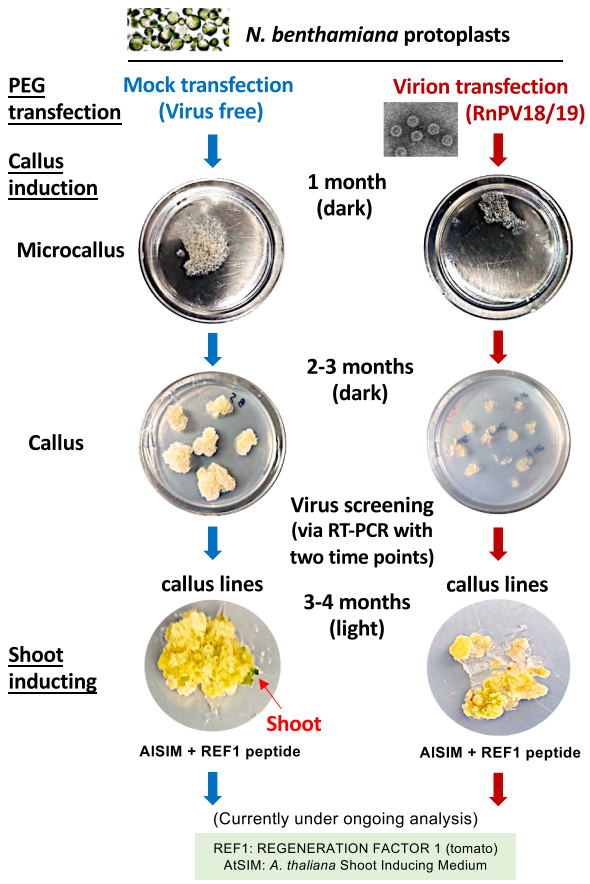

Fig. 2. Callus formation in *N. benthamiana* protoplasts transfected with two fungal partitiviruses.
Callus development was compared between cells transfected with RnPV18 and RnPV19 (right) and mock-transfected cells (left). Under dark conditions, microcallus formation required approximately one month (top row), whereas visible callus formation required a few months (middle row). As described in the Results section, transfection with the partitiviruses significantly delayed callus formation relative to the mock transfection (virus-free control). During the callus induction step, calli derived from the transfected protoplasts were screened by RT-PCR (see Fig. 3). Furthermore, shoot formation from virus-transfected calli on shoot induction medium was extremely limited compared to the mock-transfected samples (bottom row).

compare viral behavior across different plant developmental stages, including protoplasts, calli, and suspension cultures.

2. Materials and methods

2.1. Virus purification

Virus particles were purified from *Rosellinia necatrix* strain W442, which is co-infected with RnPV18 and RnPV19 (Telengech et al., 2020) as described by Das et al. (2022). Briefly, approximately 20 g wet weight of mycelia was homogenized to a fine powder in liquid nitrogen, and virus particles were extracted in 40 mL of 0.1 M sodium phosphate buffer, pH 7.0, containing 40 µl of β-mercaptoethanol. After clarification with a quarter volume of carbon tetrachloride (CCl_4). Virus particles were then precipitated in 1% NaCl and 8% PEG 6000, followed by differential centrifugation to recover and resuspend the pellets in 0.05 M PB (pH 7.0). If necessary, the virus-containing aqueous phase was subjected to differential centrifugation and sucrose density gradient centrifugation (10–50%, w/v), and the final pellet was suspended in 100 µl of 0.05 M sodium phosphate buffer.

Similarly, virus particle fractions were obtained from 20 g of transfected calli that had previously tested positive for RnPV18. The final purified fraction was examined by electron microscopy as described by Kondo et al. (2023) using a model H-7650 transmission electron microscope (Hitachi, Tokyo, Japan).

2.2. Protoplast transfection, callus induction and establishment of suspension cultures

The entire experimental procedure from protoplast preparation, virion transfection, callus formation and plantlet development (shoot induction), is shown in Fig. 1. Virus purification from *R. necatrix* strain W442 and protoplast isolation and transfection were conducted according to the method described by Telengech et al. (2024). Virion preparations were filter sterilized through a 0.22 µm mesh filter (Millipore), and the protein concentration was estimated by measuring absorbance at 280 nm. Protoplasts were isolated from 5- to 6-week-old *N. benthamiana* plants. Four fully expanded leaves were cut into ~1 mm strips, and incubated overnight (16 h) at 22 ± 2 °C in the dark in an enzyme solution comprising 1.0% (w/v) Cellulase RS and 0.5% (w/v) Macerozyme R-10 (Yakult Pharmaceutical Industry, Tokyo, Japan) in MMC buffer containing 0.5 M mannitol, 5 mM MES (pH 5.7) and 10 mM $CaCl_2$. The resulting digested tissue was filtered through four layers of sterile gauze using a Büchner funnel into a 50 mL Falcon tube. Protoplasts were pelleted by centrifugation at 46 × g for 3 min using a tabletop centrifuge (Model KN-70, Kubota Corp.), washed once with 10 mL MMC solution, and then resuspended at a density of 1×10^6 cells/mL in W5 solution (154 mM NaCl, 125 mM $CaCl_2$, 5 mM KCl, 2 mM MES, pH 5.7). The suspension was incubated on ice for 3 h prior to transfection.

For transfection, 100 µl of protoplast suspension was mixed with 10 µl of virus particles. Transfection was conducted using PEG solution (40% [w/v] PEG 4000, 0.4 M mannitol, 100 mM $Ca(NO_3)_2$) followed by dilution with 2 mL dilution buffer (0.5 M mannitol, 125 mM $CaCl_2$, 5 mM KCl, 5 mM glucose, 1.5 mM MES, pH 5.7), and the mixture was incubated on ice for 15 min. Transfected protoplasts were washed with 2 mL dilution buffer and resuspended in W5 buffer at 22 ± 2 °C. The transfected protoplasts were then washed with callus induction medium [CIM: half-strength Murashige and Skoog (MS) salts (Murashige and Skoog, 1962) and Gamborg's B5 vitamins (Gamborg et al., 1968) supplemented with 3% sucrose, 1 mg/L NAA (FUJIFILM Wako, Osaka, Japan) and 0.3 mg/L kinetin (FUJIFILM Wako)] and 0.4 M mannitol, centrifuged and finally resuspended in 200 µL CIM. Aliquots (100 µL) of the protoplast suspension were gently mixed with an equal volume of 2.8% sodium alginate (Sigma-Aldrich) in 0.4 M mannitol. The mixture was thinly layered onto $CaCl_2$-agar (20 mM $CaCl_2$, 0.4 M mannitol, and 1% agar). After 1 h incubation at room temperature, the entire thin layers were carefully removed and transferred into 6-cm Petri dishes containing 4 mL CIM containing 0.4 M mannitol. Cultures were maintained in the dark at 22 °C, with serially substituting the liquid medium with CIM without mannitol every 10 to 14 days until the formation of visible colonies (mini calli). Using sterile forceps, the colonies were transferred to CIM solidified with 0.8% agar for multiplication. Cultures were maintained in the dark and subcultured every three weeks. For shoot induction, a shoot-inducing medium for *A. thaliana* (AtSIM) (Valvekens et al., 1988) containing 1 nM REGENERATION FACTOR 1 (REF1), a regeneration-enhancing peptide (Yang et al., 2024), was tested.

To initiate cell suspension cultures, vigorously growing friable portions (a few mm in diameter) of calli were transferred into 25-mL mLS2 liquid medium in a 100-mL Erlenmeyer flask. mLS2 medium was partially modified from mLS (modified Linsmaier and Skoog) medium (Nagata et al., 1992) and consisted of MS salts and B5 vitamins supplemented with 0.2 g/L KH_2PO_4, 0.2 mg/L 2,4-D, 0.02 mg/L BAP (pH 5.8). The cultures were then incubated in the dark at 25 °C on a shaker (Bio-Shaker BR-40LF, TAITEC Corp.) at 90 rpm. The suspension cultures were maintained by subculturing ca. 1.5 mL of packed cell volume (PCV) into fresh mLS2 medium every two weeks.

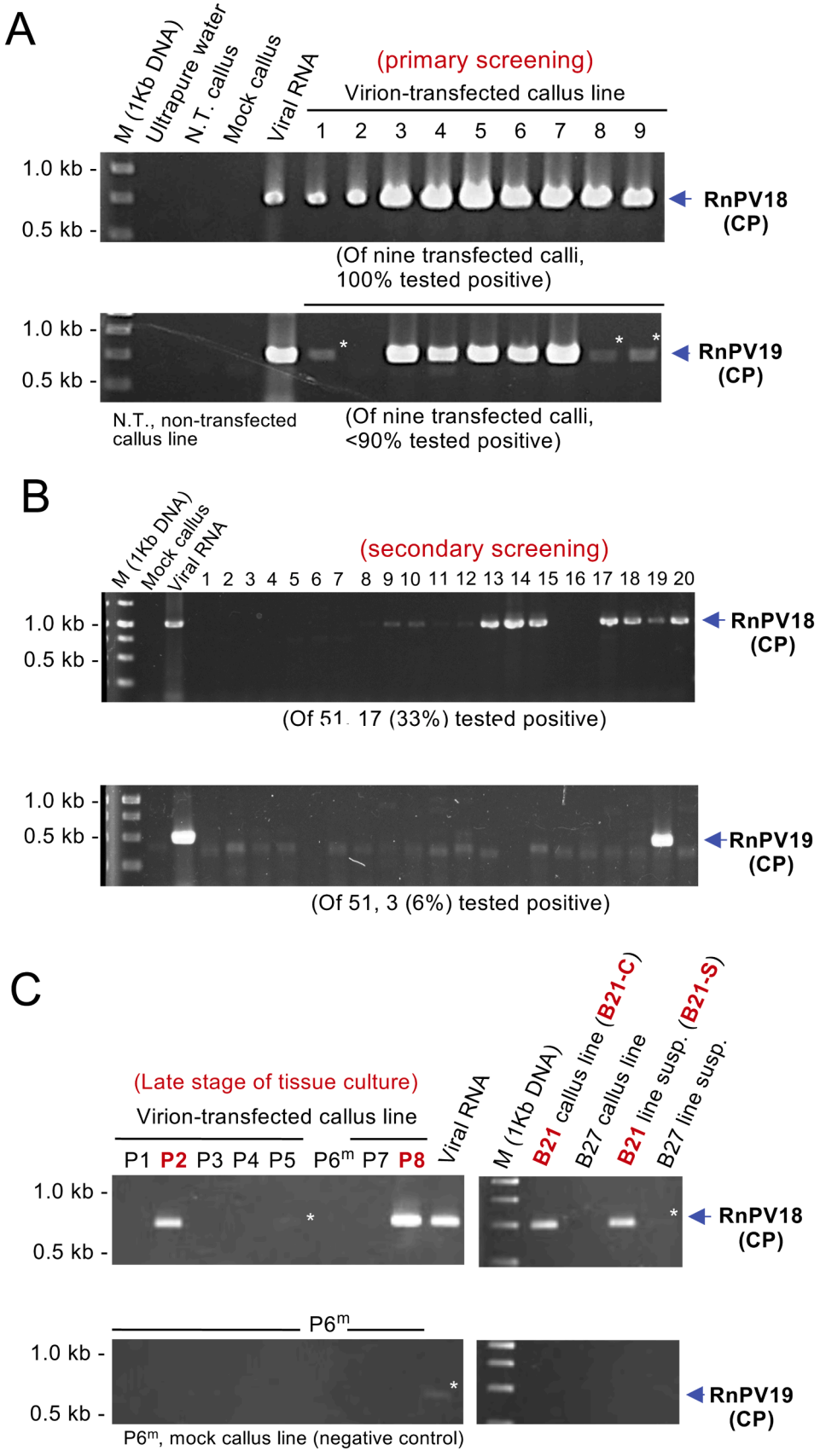

(caption on next page)

Fig. 3. Primary and secondary screening of *N. benthamiana* calli derived from transfected protoplasts by RT-PCR. **(A, B)** Primary (A) and secondary screening (B) of transfected calli. Screening was conducted by RT-PCR using the primer sets RnPV18 CP F2 and RnPV18 CP R2 (A, 491 bp) or 874F and 847R (B, 1017 bp) for RnPV18 and RnPV19 CP F2 and RnPV19 CP F2 (A and B, 503 bp) for RnPV19. Ultrapure water, non-transfected (NT) callus, mock-transfected callus (Mock) and purified viral RNA were included in RT-PCR assay in parallel. (**C**) Late-stage screening of transfected calli and their suspension cultures. RT-PCR was conducted using the same primer set as the primary screening. This was performed at a further later stage of callus development and in suspension cultures to obtain stably infected lines. The right panel of C includes representative data from suspension culture cells derived from selected virus-positive callus (B21, P2 and P8 lines). The virus detection rates are indicated in red text below each panel. Total RNA fractions and RT-PCR were prepared from generated calluses or their corresponding suspension culture cells as described in the Materials and Methods section. Calli were numbered arbitrarily and these identifiers are used consistently hereafter. The suffixes -C and -S are used to distinguish between callus and suspension culture cell samples, respectively. * refers to relatively faint RT-PCR bands, indicating virus infection.

2.3. Screening of callus and plantlet materials for virus infection

A subcultured greenish and round-shaped callus (approximately 3 mm in diameter) was minced in 500 μL of an RNA isolation reagent (RNAisoPlus, Takara-Bio, Otsu, Japan) in a 1.5-mL microtube using a disposable pestle. After repeated extraction with 100 μl of chloroform, RNA was ethanol-precipitated and resuspended in 50 μl of distilled water. For plantlets, a leaf disc of 0.5 cm in diameter was obtained from a developing leaf and used to isolate RNA in a microtube, as described above for calli.

Extracted RNA was used for RT-PCR-based detection of viral RNA as described previously by Telengech et al. (2020). The primer sets used were RnPV18 Cp F2 (5′-TAAGTTCGCTGAATACCTGCTCT −3′) and RnPV18 Cp R2 (5′-CGTTAATTGCGGAAGCTTTCTTG −3′) or RnPV18 Cp F3 (5′-GTTAACGCTGTCTACGCTACT-3′) and RnPV18 Cp R3 (5′-GTTAGAGGTCTTGGTCATACC-3′), and RnPV19 Cp F2 (5′-GCGCATCAGCTTTACTTCTCAATT-3′) and RnPV19 Cp R2 (5′-GCATTGATCTCGGTATTACTCC-3′) or RnPV19 RdRP F1 (5′-ACGAATCTTCCGAACCCCTC-3′) and RnPV19 RdRP R1 (5′-CCATGTTGTAGAGGGAGTCAA-3′) for RnPV18 and RnPV19, respectively.

For Sanger sequencing of RnPV18 dsRNA1 in suspension cell cultures, RT-PCR fragments were amplified using the primer set RnPV18_SC_F_59 (5′-CCCGCAAAGAACAAGTCCTC-3′; nt 693–712) and RnPV18_SC_R_59 (5′-GTCATAGCCGGACCAGTCAA-3′; nt 1280–1299). After cloning into the pGEM-T Easy vector (Promega, Madison, WI, USA), individual cDNA clones were subjected to Sanger sequencing using a BigDye Terminator v3.1 Cycle Sequencing Kit (Thermo Fisher Scientific Inc.).

2.4. RNA analyses

Total RNA fractions were obtained from solid calluses and liquid suspension cultures. Relatively young, 3- to 5-week-old calluses and suspension cultures were homogenized using a mortar and a pestle in the presence of liquid nitrogen. A bulk of 20 calli of approximately 50 mm^3 each (about 1 g in total) for each line was harvested and minced in 10 mL of extraction buffer (STE-SDS) containing 20 μl of 2-mercaptoethanol (Suzuki and Nuss, 2002) and phenol/chloroform/isoamyl alcohol (IAA). For suspension cultures, a total of 25∼30 mL suspension cultures for each line were filtered through miracloth, washed with twice with sterile water, and homogenized in 10 mL of extraction buffer. Total ssRNA was enriched by the LiCl method as described by Shahi et al. (2025) after extraction with phenol, phenol/chloroform, and chloroform IAA. RNA was further purified following RQ1 DNase (Qiagen, Hilden, Germany) treatment. Total RNA fractions were used in northern blotting as described Sato et al. (2022), and sent to Genome-Lead Inc. (Takamatsu, Kagawa, Japan) and Macrogen Inc. (Tokyo, Japan) for high-throughput total RNA and small RNA sequencing, respectively. For RNA-seq, rRNA-depleted, DNase-treated total RNA fractions were used for library preparation in Genome-Lead Inc. using an MGIEasy Fast RNA Library Prep Set, and sequenced on an MGI platform in 150-bp pair-end mode. For sRNA-seq, a library was prepared using an NEBNext Small RNA Library Prep Set for Illumina Kit, and sequenced on an Illumina platform in 50-bp single-end mode. Northern blotting was according to the method of Sato et al. (2022). RNAs, which were electrophoresed in 1 x MOPS (3-morpholinopropanesulfonic acid) buffer system, were transferred to a nylon membrane (Hybond-N^+, GE healthcare Inc.), and probed using cDNA probes labelled by Digoxigenin (DIG)-11-dUTP and antibody against DIG (F. Hoffmann-La Roche, Ltd.). The DIG-labelled probe was amplified using a PCR primer set (PV18_RNA1–1000F: 5′-TCTGATGAACAAGTCCGCGATTAT-3′ and RNA1–2000R: 5′-ACATAGTGTAAATATCGTTGCAAA-3′) which targets RnPV18 dsRNA1 specifically.

2.5. Bioinformatics analyses of RNA and small RNA sequences

Total RNA-seq data were adapter and quality-trimmed using fastp (Chen, 2025) with manufacturer-provided adapter sequences and the option –trim_poly_g. Trimmed reads were mapped against a combined reference consisting of the *N. benthamiana* reference genome (v2.6.1 – SolGenomics) and RnPV18 sequences deposited in GenBank (LC517384.1, LC517385.1) using HISAT2 (Kim et al., 2019). SAMtools (Li et al., 2009) was used for sorting, indexing and calculating coverage statistics. Counts per million were extracted using FeatureCounts (Liao et al., 2014) and a custom script for specific calculation. Small RNA-seq data were similarly trimmed using fastp (Chen, 2025) with the option –length_required 18 and –length_limit 30. Mapping was performed using bowtie v1 (Langmead et al., 2009) and coverage data were obtained using BEDTools genomecov (Quinlan and Hall, 2010). Single nucleotide polymorphisms (SNPs) were identified with LoFreq (Wilm et al., 2012) with the –no-default-filter parameter. Functional annotation of variant was performed using SnpEff (Cingolani et al., 2012). All statistical analyses and data visualization were performed in R (v4.4.2). VCF files were parsed using vcfR (v1.16.0). Data manipulation was handled via dplyr (v1.1.4) and tidyr (v1.3.1). Plots were generated using ggplot2 (v4.0.2), patchwork (v1.3.2), and ggrepel (v0.9.8).

3. Results

3.1. Screening for partitivirus-positive calli

Numerous calli were obtained from both virus-transfected and mock-transfected protoplasts of *N. benthamiana*. Notably, callus development was generally delayed in protoplasts transfected with the two partitiviruses compared with mock-transfected, virus-free protoplasts (Fig. 2). *R. necatrix* strain W442 is co-infected with two partitiviruses, RnPV18 (betapartitivirus) and RnPV19 (alphapartitivirus) (Telengech et al., 2020). Previous work has shown that *N. benthamiana* supports replication of the betapartitivirus more efficiently than that of the alphapartitivirus at the protoplast level (Telengech et al., 2024).

RT-PCR analysis performed 11 weeks post-transfection showed that all 9 tested calli were positive for RnPV18, whereas 8 of 9 (∼90%) were positive for RnPV19 (Fig. 3A). In contrast, none of the calli derived from mock-transfected protoplasts were positive for either virus. In a previous study using carrot protoplasts transfected with the same virus combination, no RnPV19-positive calli were obtained (Telengech et al., 2024). These observations suggest that *N. benthamiana* is more permissive to fungal partitiviruses than carrot.

After six months of subculturing, secondary screening was conducted. Only 3 of 51 calli (6%) remained positive for RnPV19 (Fig. 3B). In contrast, 17 of 51 calli (33%) retained RnPV18 infection, whereas the

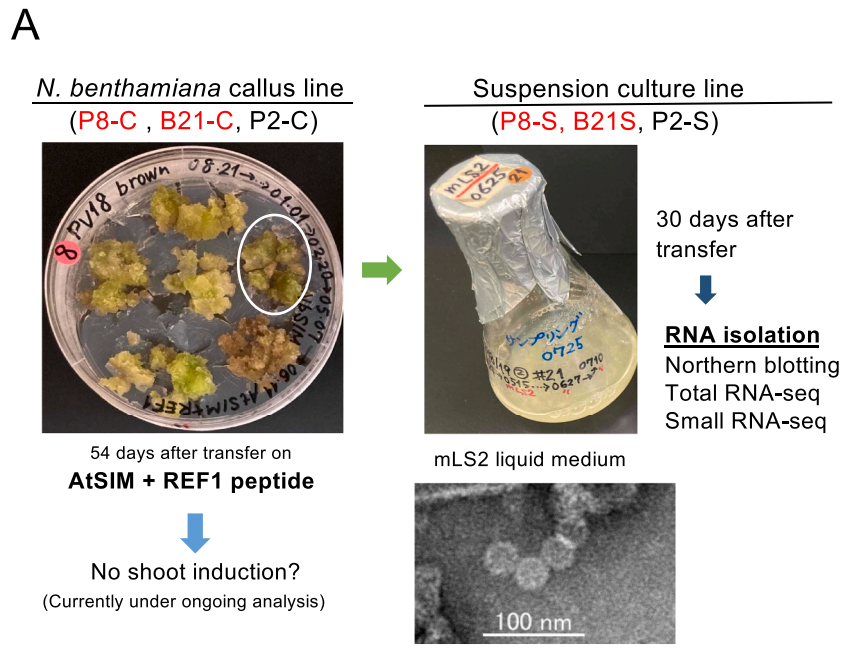

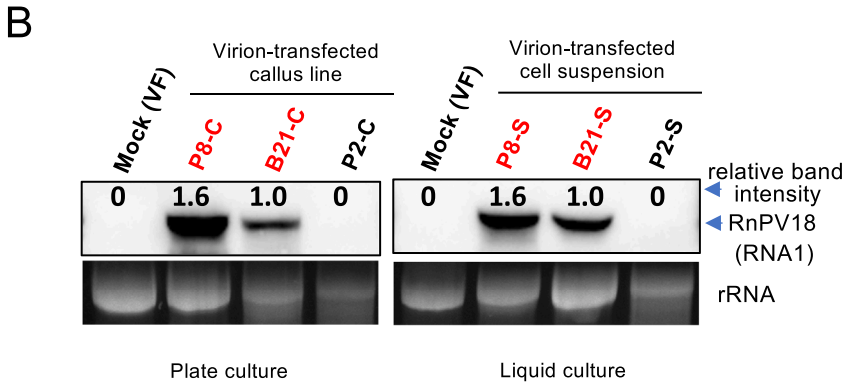

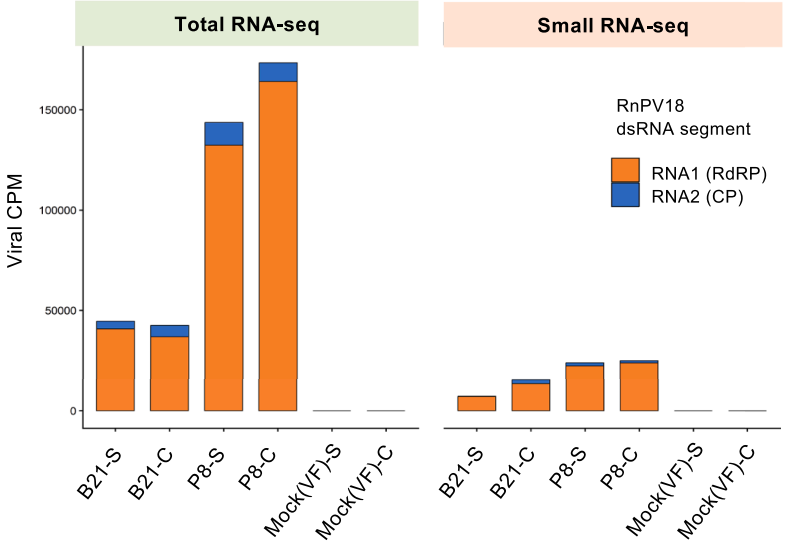

(caption on next page)

Fig. 4. Stably infected *N. benthamiana* callus lines with RnPV18 derived from transfected protoplasts and repeated subculture.
(A) Development of stably infected tissue culture lines. After the secondary screening, several independent RnPV18-positive calli were maintained to stable infectants. Two stably infected lines (P8 and B21) were selected, after repeated subculture. These calli termed P8-C and B21-C were used to establish suspension cultures (P8-S and B21-S) (right panel). The P2 callus line (P2-C) and its P2-S suspension culture were also included as an unstable RnPV18 infectants. RnPV18 infection was confirmed by RT-PCR, as shown in Fig. 3. The transmission electron micrograph (TEM) showing spherical RnPV18 particles approximately 30 nm in diameter in the semi-purified fraction from the P8 line. **(B)** Northern blotting of selected tissue culture lines. Total RNA was isolated from a total of eight cultures: mock transfected calli, P8-C, B21-C, P2-C, mock-transfected suspension culture, P8-S, B21-S, and P2-S. These RNA samples were subjected to northern blotting with DIG-labelled cDNA probe specific for RnPV18 dsRNA1. Note that while P2 was an unstable infectant line, P8 and B21 were stably infected lines. The large ribosomal 28S RNA was used as a loading control. The intensities of the specific northern blot signals were quantified using ImageJ after normalization to the rRNA bands. Relative values normalized to the B21 line (set to 1.0) are shown. **(C)** High-throughput sequence analyses of total RNA and small RNAs (sRNAs). Two RNA fractions were obtained from each of the six cell lines: calli (mock transfected, P8-C, and B21-C) and suspension culture cells (mock-transfected, P8-S, and B21-S). Viral counts per million (CPM) were calculated from total RNA or sRNA data (see also Fig. 5–7) and mapped to RnPV18 genome (comprising combined dsRNA1-RdRP and dsRNA2-CP), comparing the four different stably infected lines. Mock-transfected callus samples were also included in these analyses as negative controls. See Materials and Methods for data acquisition and bioinformatic analyses.

Table 1
High-throughput small RNA sequencing data on RnPV18-infected tissue culture lines.

Sample	dsRNA1 Count	dsRNA2 Count	Total Mapped Count	Total Viral Counts	Viral_CPM
B21_S	646,654	59,874	15,834,107	706,528	44,621
B21_C	776,257	118,545	21,051,300	894,802	42,506
P8_S	4,319,663	368,920	32,632,100	4,688,583	143,680
P8_C	3,198,839	180,372	19,426,100	3,379,211	173,952
VF_S	564	42	19,407,500	606	31
VF_C	188	15	9,489,080	203	21

remainder were virus-free (Fig. 3B). These results indicate that RnPV18 is maintained more stably than RnPV19 during proliferation of *N. benthamiana* cultured cells.

Twenty two-month-old calli were randomly selected, and used for weight measurement. Callus weight was 208 ± 143 (SD) mg/callus for RnPV18-transfectants and 458 ± 234 (SD) mg/callus for mock-transfectants. A weight reduction by virus transfection, relative to mock-transfection, was statistically significant ($p < 0.0005$) when assessed using the Mann–Whitney U test. These align with the observations shown in Fig. 2 and suggest that RnPV18 infection negatively influences callus growth and development.

3.2. Establishment of fungal partitivirus-positive calli and suspension cultures

Calli were further propagated in an attempt to regenerate plantlets (see Figs. 1 and 2), and viral presence was periodically examined. Some calli retained RnPV18 even after prolonged subculturing (>10 passages, approximately 9–10 months. Several RnPV18-positive calli were subsequently used to establish suspension cultures by a conventional method. During secondary RT-PCR screening (Fig. 3B), subcultures derived from a single callus occasionally showed discordant results, with both RnPV18-positive and -negative outcomes (e.g., B27 lines in Fig. 3C, right panel). This indicates that individual calli can exhibit a chimeric nature, consisting of both virus-infected and virus-free cells.

To assess long-term stability, ten calli that had been subcultured every 1–2 months were randomly selected, and some were confirmed to retain RnPV18 (Fig. 3C, left panel). Virus-positive calli were transferred to liquid medium to establish suspension cultures. Total RNA was extracted from both suspension cultures and their corresponding calli and analyzed by northern blotting (see also Fig. 1). Two independent lines, P8 and B21, were selected for further analysis. Suspension cultures (P8-S and B21-S) and calli (P8-C and B21-C) derived from these lines retained RnPV18 after approximately 10 passages (~9 months post-transfection). Northern blot analysis confirmed the presence of RnPV18 in both P8-C and P8-S, whereas no virus-specific signals were detected in negative controls (Fig. 4A), demonstrating stable maintenance of RnPV18 in calli and suspension cultures of *N. benthamiana*. Importantly, we could observe RnPV18 particles approximately 30 nm in diameter in semi-purified fractions from line P8 (Fig. 4A).

Although the calli termed P8-C and B21-C, and suspension cultures designated P8-S and B21-S showed stable RnPV18 infection, they showed different levels of virus content, as estimated by northern blotting and total RNA sequencing (see Fig. 4B and C). The virus content appears to be lower in B21 than in P8, regardless of whether the virus was maintained in calli or suspension cultures. B21-C and B21-S shared the same origin, meaning they were derived from a single transfectant, as was in the case for P8-C and P8-S, as shown below. Viral transcript levels were empirically estimated to be on the order of several to several tens of pg per mg of calli, according to our northern detection system. However, these estimates must be validated after establishing a standard curve using in vitro synthesized RnPV18 transcripts.

3.3. Distinct virus-derived small RNA profiles across developmental stages

We previously reported differences in viral small interfering RNA (vsiRNA) profile among fungal colonies, cultured insect cells, and plant protoplasts, which were infected systemically or at the cellular level by RnPV18 (Telengech et al., 2024). We were interested in investigating how different or similar RnPV18-derived small RNA (sRNA) accumulation among RnPV18-infected cells, tissue cultures, and organisms were. For this purpose, we obtained sRNA sequence data from four samples in this study: RnPV18-infected P8-S, B21-S, P8-C and B21-C, in addition to two virus-free control samples (Table 1). Previously obtained data from RnPV18-transfected protoplasts (Telengech et al., 2024) were re-analyzed for comparison (Figs. 5 and 6, top panels).

Comparative analyses revealed both shared and distinct features. Across all developmental stages, RnPV18-derived sRNAs from both dsRNA1 and dsRNA2 showed a dominant peak at 21 nt. However, this peak was sharper in protoplasts than in calli and suspension cultures, particularly in B21-S (Fig. 5A and B). Similarities extended to the 5′ nucleotide preference and the larger amounts of dsRNA1-derived sRNAs compared to dsRNA2-derived sRNAs. Uridine (U) and adenosine (A) were the predominant 5′ nucleotides across all samples (Fig. 5C and D). This bias was more pronounced in 20- and 21-nt sRNAs from calli and suspension cultures (over 75% except for one case, B21-C, Fig. 5C and D), relative to those from protoplasts (below 60%) (Fig. 5C and D, top panel). Furthermore, dsRNA1-derived sRNAs were consistently more abundant than dsRNA2-derived sRNAs, with a difference exceeding sixfold. Strand bias differed markedly among stages. In calli and suspension cultures, sRNAs derived from positive-sense strands predominated (>64%), whereas in protoplasts the opposite trend was observed (<49%) (Fig. 5A and B), consistent with previous findings (Telengech et al., 2024).

Clear differences were observed in sRNA mapping profiles. Calli and suspension cultures showed highly similar mapping patterns, with peaks at conserved positions along both dsRNA segments (Fig. 6A and B). In contrast, protoplast-derived sRNAs displayed distinct profiles. For example, a prominent peak at approximately position 2300 on the

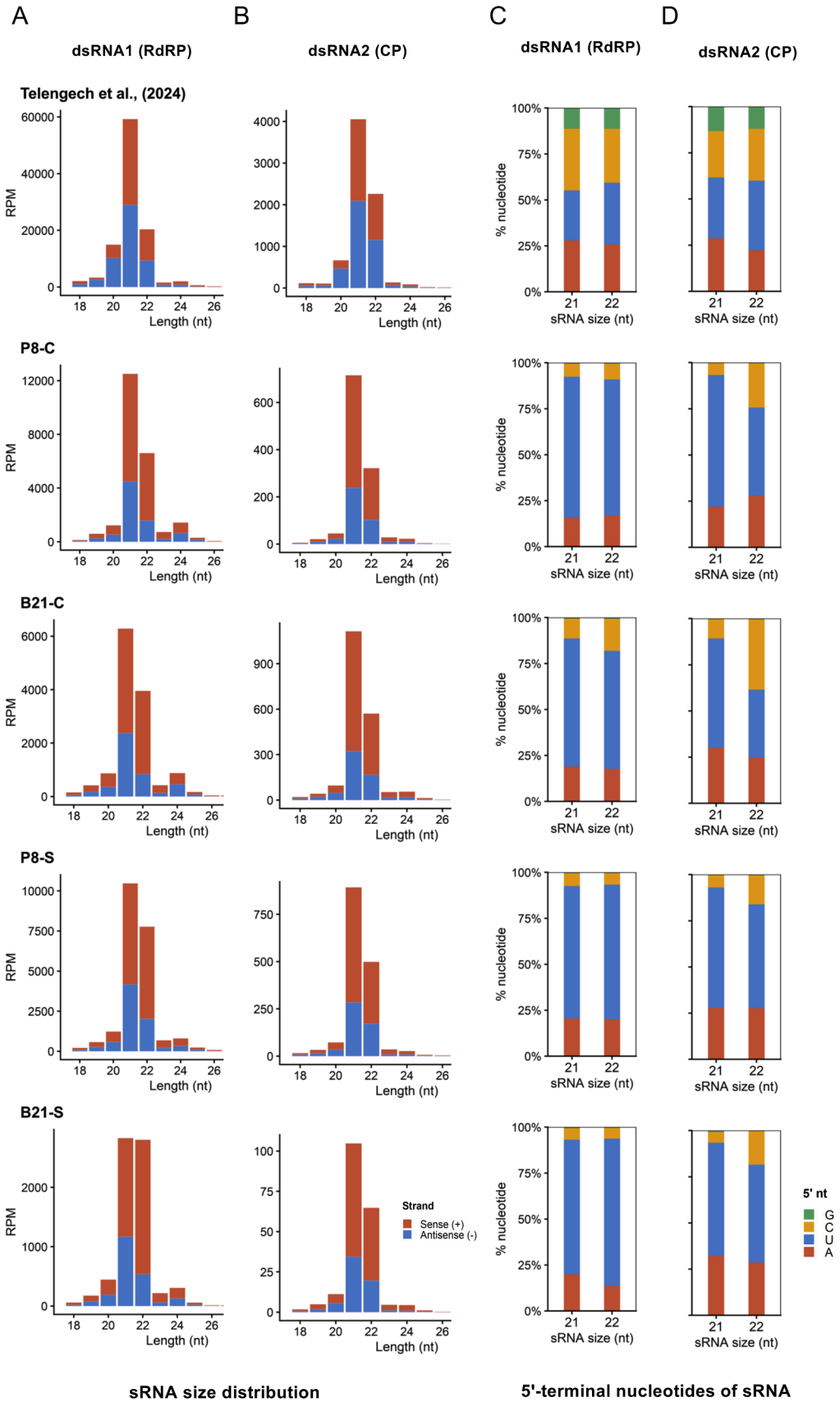

(caption on next page)

Fig. 5. Small RNA profiles derived from RnPV18 dsRNA1 in RnPV18-infected *N. benthamiana* protoplasts, calli and suspension cultures. Small RNA (sRNA) fractions were obtained from four tissue culture samples of stably infected lines: RnPV18-positive callus lines P8-C and B21-C, and RnPV18-positive suspension culture lines P8-S and B21-S. These were then sequenced using high-throughput sequencing technologies. The sRNAs derived from RnPV18 dsRNA1 (A, C) and dsRNA2 (B, D) were analyzed in terms of their size distribution (18–26 nts, A, B), and their 5′ nucleotide for 21- and 22-nt reads (C, D). The sRNAs from the positive-sense and negative-sense RNAs are shown in red and blue, respectively (A, B). The RnPV18-derived sRNAs in transfected protoplasts, for which raw read data were obtained previously from transfected *N. benthamiana* protoplasts (Telengech et al., 2024), were also analyzed in parallel (top panels).

positive strand of dsRNA1 was observed in protoplasts (Fig. 6A, top left panel) but not in calli or suspension cultures (Fig. 6B). Moreover, protoplast-derived sRNAs exhibited a more uniform, genome-wide distribution, particularly for dsRNA2 (Fig. 6B top, right panel). These patterns may represent signatures of early-stage viral replication following transfection.

3.4. Line-specific differences in viral accumulation and sequence variation

Another notable finding was the difference in viral accumulation and sequence heterogeneity between the P8 and B21 lines. RnPV18 accumulated at higher levels in P8 than in B21, as measured by total RNA-seq counts per million (CPM) (see Fig. 7). This difference was consistent across both calli and suspension cultures. We next examined sequence variation in RnPV18 populations across developmental stages. A striking feature was the accumulation of a nonsense C-to-U mutation at position 1010 within the RdRP coding region in B21-derived samples. This mutation was present in approximately 50% of reads in B21-C and at even higher frequencies in B21-S (Fig. 7A). This substitution was validated by Sanger sequencing of RT-PCR fragments spanning position 1010 after being cloned into pGEM-T easy. Among 12 cloned cDNA fragments from the B21 suspension culture, 6 (50%) carried the mutation, whereas none of the five clones from the P8 suspension culture contained this substitution (Fig. 8). The C-to-U mutation introduces a premature stop codon, likely resulting in a truncated RdRP protein and reduced viral replication efficiency in the B21 line. Notably, this mutation was not detected in RnPV18 sequences derived from the original fungal host or from the regenerated carrot plants in previous studies (Telengech et al., 2020, 2024 and unpublished data) (see Fig. 8). In addition, a non-synonymous G-to-A mutation at position 434 of dsRNA1 was present at 100% frequency in all reads, whereas a synonymous C-to-A mutation at position 1466 of dsRNA2 showed stage-specific accumulation.

4. Discussion

An increasing number of fungal viruses have been shown to replicate in organisms belonging to different kingdoms, including plants. These findings suggest that host switching may have occurred during viral evolution or may still occur among extant viruses between the kingdoms Fungi and Plantae (Andika et al., 2023; Roossinck, 2019). However, only a limited number of fungal viruses have been shown to infect new experimental hosts systemically. Valsa mali negative-strand RNA virus 1 (Dai et al., 2024) and cucumber mosaic virus (Andika et al., 2017) are among the few examples capable of naturally shuttling between plant and fungal hosts. Diaporthe sojae circular DNA virus 1 also highly likely shuttles between fungi and plants (Wang et al., 2024).

Partitiviruses are particularly intriguing in this context because single genera accommodate both plant and fungal viruses, implying historical or ongoing horizontal virus transfer between the two kingdoms. Although replication of fungal partitiviruses has been demonstrated in plant protoplasts (Nerva et al., 2017; Telengech et al., 2024), their maintenance at the tissue or whole-plant level has been achieved only in limited cases, such as carrot (Telengech et al., 2024). In this study, we demonstrate that a fungal partitivirus, RnPV18, can be stably maintained in calli and suspension cultures derived from *N. benthamiana* protoplasts (Figs. 1–4), which allowed us to study RnPV18 behaviors at different developmental stages (Figs. 5–8). This represents an important step toward establishing an *in planta* experimental system for persistent fungal viruses. In addition, the combination of virion transfection and plant tissue culture described here may be broadly applicable to other persistent plant and fungal viruses, which are typically difficult to inoculate experimentally.

Despite successful establishment of RnPV18 infection in calli and suspension cultures, regeneration of whole plants from infected tissues was severely impaired. In contrast, mock-transfected, virus-free protoplasts readily regenerated into plantlets (Fig. 2 and data not shown). These observations suggest that RnPV18 infection interferes with one or more key growth steps required for plant regeneration, such as callus proliferation, shoot induction, or root formation. Consistent with this idea, we previously observed that carrot plants regenerated from RnPV18-transfected protoplasts exhibited systemic infection but failed to produce seeds (Telengech et al., 2024), indicating that persistent fungal viruses may affect plant development even in the absence of overt symptoms. Future studies using *N. benthamiana* mutant lines, particularly those defective in antiviral RNA silencing pathways, may help determine whether host defense responses contribute to these developmental defects. To perform *in-planta* study of RnPV18 in *N. benthamiana,* the above-mentioned growth problem (shooting and probably other steps) should be solved. Once RnPV18-infected plants are obtained, many open questions will be answered. Example questions include: Can fungal partitiviruses be targeted by RNAi in planta? Can fungal partitiviruses move systemically and locally? Can fungal partitiviruses be transmitted thorough seeds like plant partitivirues? Can fungal partitiviruses be inoculated mechanically or via vector organisms? Can this method apply to other persistent plant and fungal viruses?

Small RNA sequencing provided further insights into host–virus interactions at different growth stages. A striking observation was that sRNAs derived from the RdRP-encoding dsRNA1 accumulated at substantially higher levels than those derived from the CP-encoding dsRNA2 (Fig. 5A and 5B). Factors influencing the ratio of dsRNA1-derived to dsRNA2-derived sRNAs may include viral transcript abundance, the accessibility of Dicer-like proteins to viral RNA substrates, and culture conditions that potentially alter RNA silencing activity. Although similar trends have been reported in some fungal systems (Ozkan et al., 2017), other studies have shown comparable accumulation of sRNAs from the two genomic segments (Jiang et al., 2023). These discrepancies may reflect differences in host species, virus strains, or physiological conditions. Because a single partitivirus particle comprises 60 CP homodimers, one or two RdRP molecules and one genomic segment, either dsRNA1 or dsRNA2 (Ghabrial et al., 2015; Mata et al., 2020), it is generally expected that CP-related transcripts or genomic segments would accumulate more abundantly. In consistent with this, much greater accumulation of CP-encoding transcripts and genomic dsRNA have also been reported for some *Heterobasidion* (basidiomycetous fungus) partitiviruses in the original host (Jurvansuu et al., 2014). However, previous studies have shown that the relative abundance of dsRNA segments can vary depending on host–virus combinations and growth conditions (Chiba et al., 2013; Jurvansuu et al., 2014; Velasco et al., 2020). In fact, our preliminary experiments using regenerated carrot plants (Telengech et al., 2024) showed that the levels of RnPV18 segment accumulation were comparable (see Fig. 7A and B, top panels, P. Telengech, H. Kondo, and N. Suzuki, unpublished data). There must be some mechanisms that control the ratio of dsRNA1 transcripts/sRNAs vs. dsRNA2 transcripts/sRNAs. Although there was a degree of correlation between sRNA levels and viral titers in both the B21 and P8 lines,

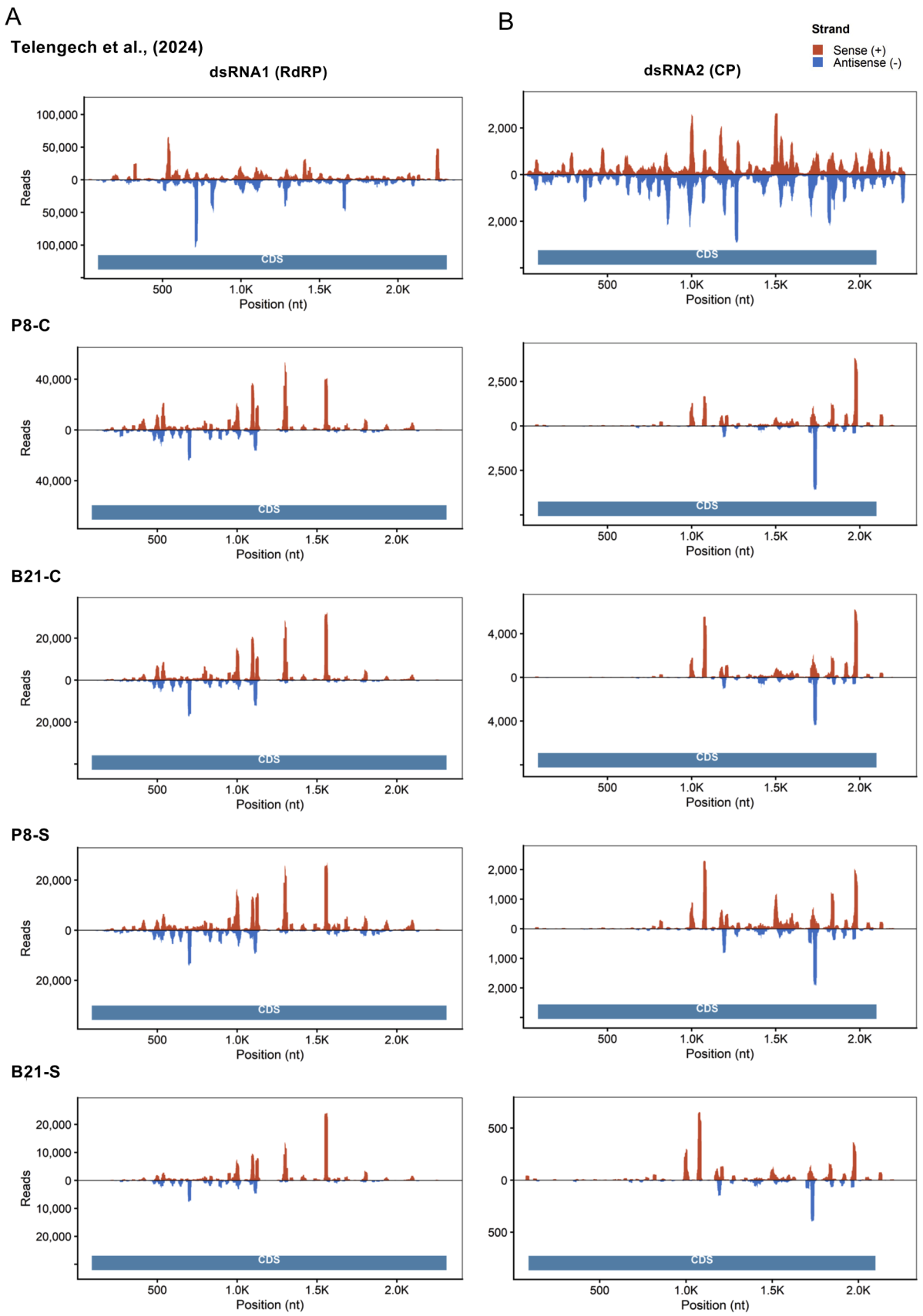

Fig. 6. Mapping of small RNAs to RnPV18 dsRNA1 and dsRNA2.
(A, B) Mapping of small RNAs (sRNAs) to RnPV18 dsRNA1 (A) and dsRNA2 (B). Small RNA (sRNA) fractions were obtained from four tissue culture samples (see the Fig. 5 legend) and analyzed together with previously obtained sRNAs from transfected *N. benthamiana* protoplasts (Telengech et al., 2024) (top panels).

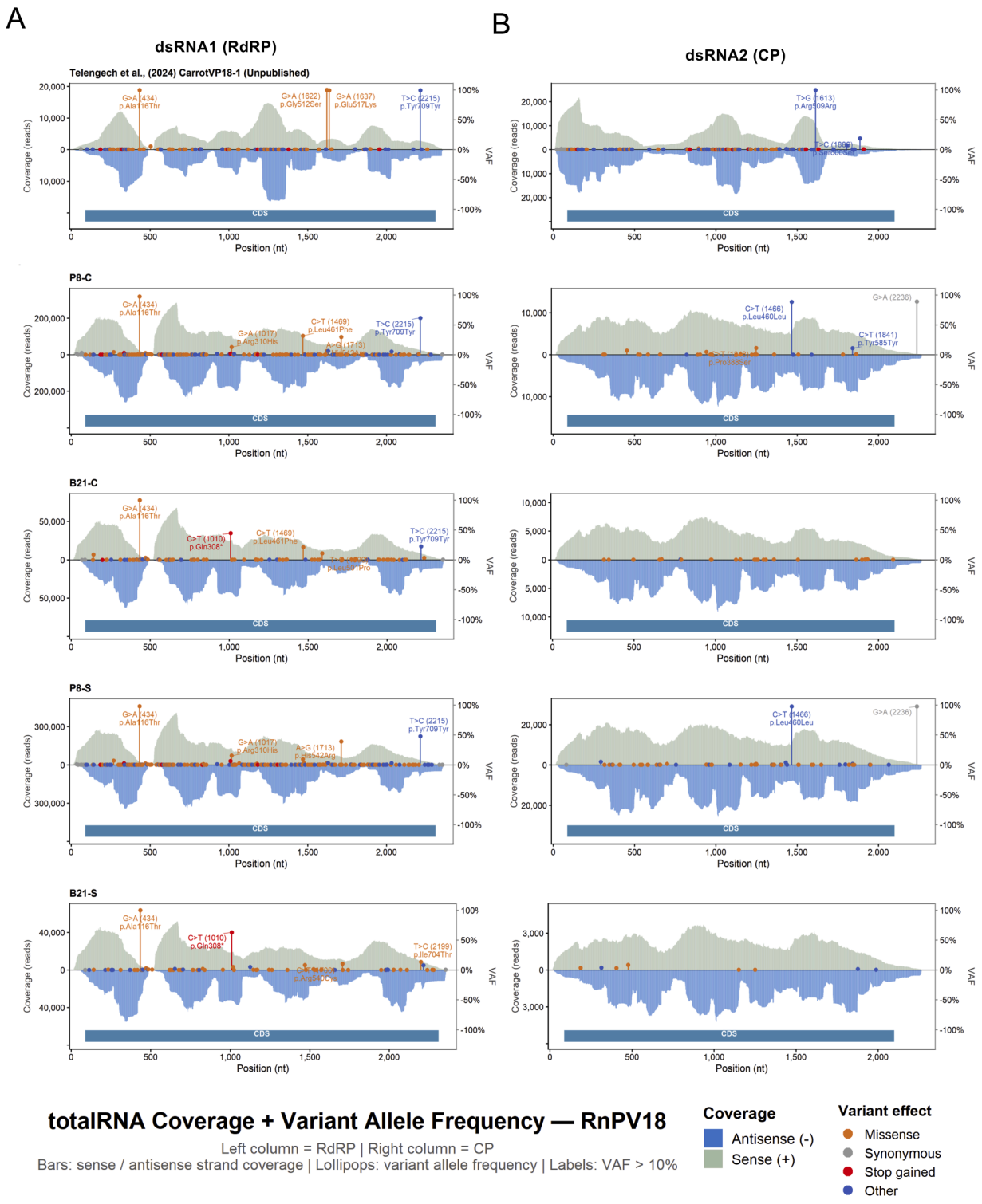

Fig. 7. Density of RnPV18-derived total RNA-seq reads along the dsRNA genomic segments and mutation frequency. Total RNA-seq data were analyzed for the same four stably RnPV18-infected lines as in Fig. 5. Read coverage across the RnPV18 genomic segments is reported for dsRNA1 (RdRP) (A) and dsRNA2 (CP) (B). The aligned reads are separated according to their coverage on the sense (green) or antisense (blue) strand. Read density of RnPV18-derived RNA-seq reads was analyzed as described in the Materials and Methods section. Variant Allele Frequencies (VAFs) from the original RnPV18 genomic sequence reported in 2020 (Telengech et al., 2020) are presented as percentages, and mutations with VAFs above 10% are labelled. The RnPV18-derived RNA-seq reads in regenerated carrot plant samples (carrot VP18-1), the raw data have been deposited in the DDBJ/EMBL/GenBank under accession number DRR1055353 (P. Telengech, H. Kondo, and N. Suzuki, unpublished data), were also analyzed in parallel (A and B, top panels).

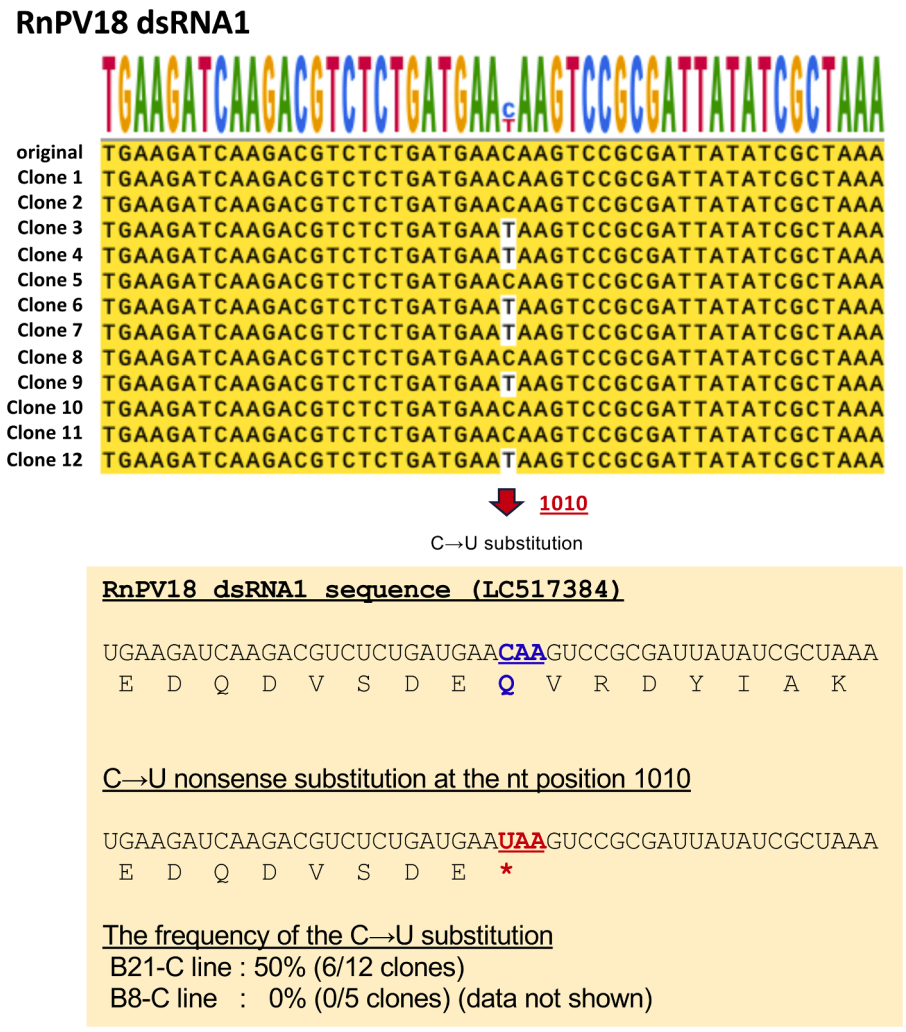

Fig. 8. Verification of the nonsense mutation at the position 1010 of RnPV18 dsRNA1 by Sanger sequencing. RT-PCR fragments spanning at position 1010 of dsRNA1 were amplified from two stably RnPV18-infected suspension cell lines (B21-S and P8-S) using the primer set RnPV18_SC_F_59 and RnPV18_SC_R_59. Following cloning into pGEM-T Easy, cDNA clones from B21-C ($n = 12$) and P8-C ($n = 5$) were subjected to Sanger sequencing. Representative sequences of the 12 clones derived from B21-C are shown. As indicated in the lower panel, the wild-type nucleotide at position 1010 in the RdRP-encoding region is C (Accession No. LC517384), whereas the introduced nonsense mutation at this site is U, resulting in a 'UAA' stop codon. Sequencing results for the two suspension cell lines are presented.

the difference in sRNA abundance was less pronounced than that in viral accumulation (Fig. 5A and B), which could suggest a bottleneck in sRNA production. Furthermore, when considering the RdRP mutant-containing viruses in the B21 line, sRNA accumulation differed between callus and suspension cultures (Figs. 5–7). These results may suggest that culture conditions can modulate viral sRNA biogenesis, particularly in the context of specific viral populations including mutations. Further replication studies are needed to clarify these speculations.

Another notable feature was the clear difference in vsiRNA profiles between protoplasts and tissue cultures. Protoplast-derived vsiRNAs exhibited broader, more uniform mapping across the viral genome particularly dsRNA2, whereas those from calli and suspension cultures showed more defined peaks at specific positions (Fig. 6). This difference may reflect distinct stages of infection: protoplasts represent an early phase following transfection, whereas calli and suspension cultures represent more established infections. The more global distribution of sRNAs in protoplasts may therefore represent a signature of initial viral recognition and processing by host RNA silencing machinery.

A key finding of this study was the identification of a line-specific nonsense mutation in the RdRP coding region of RnPV18 (Fig. 8). In natural fungal strains or following transfection into new fungal hosts, defective genome rearrangements have been reported in the RdRP-encoding segment of other *Rosellinia* partitiviruses (Chiba et al., 2013, 2016). However, such nonsense mutations have not been observed in other partitiviruses, nor have they been detected in the original fungal host, *R. necatrix*, even after prolonged maintenance (N. Suzuki, unpublished data). The C-to-U substitution at position 1010 was detected at high frequency in the B21 line but was absent in the P8 line and in the original fungal host. This mutation introduces a premature stop codon, likely resulting in a truncated RdRP protein and reduced viral replication efficiency, consistent with the lower viral accumulation observed in B21. The emergence of this mutation specifically in plant-derived cultures suggests that RnPV18 may undergo adaptive or maladaptive changes in response to the plant cellular environment. The mechanism underlying this C-to-U mutation (Fig. 8) remains unclear. One possibility is that it arises from intrinsic error-prone replication by the viral RdRP. Alternatively, host-mediated RNA editing may contribute to its generation. In animals, APOBEC family enzymes catalyze cytidine deamination and play important roles in antiviral defense against RNA viruses (Fehrholz et al., 2012; Kim et al., 2022; Kockler et al., 2026). Although canonical APOBEC homologs have not been identified in plants,

plant-specific RNA editing systems or deaminase activities have been reported (Takenaka et al., 2013). Future studies using infectious cDNA clones or in vitro replication systems will be required to distinguish between host-driven editing and replication errors. Also, it would be interesting to examine whether RnPV18 dsRNA1 transcripts with the nonsense mutation undergo nonsense-mediated decay (NMD) (Ohtani and Wachter, 2019) or whether genes associated premature termination codon-mediated NMD such as Sup35 homologs (translation termination factor eRF3) undergo somaclonal mutation in B21.

Finally, our results highlight the dynamic nature of viral populations during cross-kingdom infection. The observed differences in viral accumulation, mutation frequency, and sRNA profiles between lines and growth stages (Figs. 5–7) suggest that both host environment and cellular context strongly influence viral evolution and stability. Further studies incorporating additional biological replicates and experimental systems will be necessary to validate these findings and to dissect the underlying mechanisms.

In conclusion, this study establishes a tissue culture–based experimental platform for investigating persistent fungal viruses in a model plant system. This approach opens new avenues for studying cross-kingdom virus–host interactions, viral adaptation, and antiviral defense mechanisms in plants, and may ultimately facilitate the growth of *in planta* systems for persistent viruses that have thus far remained experimentally intractable.

Declaration of generative AI and AI-assisted technologies in the manuscript preparation process

During the preparation of this work the authors used Claude (claude-sonnet-4–6, Anthropic, accessed via claude.ai) to assist in developing bioinformatics analysis pipelines and write R scripts for variant calling, discordance analysis, and data visualization. After using this tool, the authors monitored, reviewed and edited the content as needed and take full responsibility for the content of the published article. ChatGPT (OpenAI) was used for grammatical editing of the main text.

Data deposition

Total RNA-seq and small RNA-seq data are deposited in the DDBJ/GenBank/EMBL databases with run nos. DRR1055341-DRR1055355 (BioProject: PRJDB42369).

CRediT authorship contribution statement

Paul Telengech: Writing – review & editing, Writing – original draft, Visualization, Methodology, Investigation, Conceptualization. **Sakae Hisano:** Writing – review & editing, Writing – original draft, Visualization, Methodology, Investigation, Formal analysis, Data curation. **Francesco Favaretto:** Writing – review & editing, Writing – original draft, Methodology, Investigation, Formal analysis. **Hiroaki Ichikawa:** Writing – review & editing, Writing – original draft, Methodology, Investigation, Formal analysis, Data curation. **Kazuyuki Maruyama:** Writing – review & editing, Methodology, Investigation, Formal analysis. **Kiwamu Hyodo:** Writing – review & editing, Methodology, Investigation. **Hideki Kondo:** Writing – review & editing, Writing – original draft, Visualization, Validation, Methodology, Investigation, Funding acquisition, Formal analysis, Data curation. **Nobuhiro Suzuki:** Writing – review & editing, Writing – original draft, Investigation, Funding acquisition, Formal analysis, Data curation, Conceptualization.

Declaration of competing interest

The authors declare no conflict of interests.

Acknowledgements

This work was partly supported by the Joint Usage/Research Center, Institute of Plant Science and Resources, Okayama University, the Ohara Foundation for Agriculture Research, JSPS KAKENHI Grant Numbers 16H06436, 16H06429, 16K21723, 21H05035, 25K21734, and 26K21759 (to NS and HK), 23H02214 and 23K18029 (to HK and NS). Dr. Yuta Isobe and Ms. Hitomi Sugawara (IPSR, Okayama University) are greatly acknowledged for her invaluable technical assistance.

Data availability

Data will be made available on request.

References

Andika, I.B., Maruyama, K., Sun, L., Kondo, H., Tamada, T., Suzuki, N., 2015. Differential contributions of plant Dicer-like proteins to antiviral defences against potato virus X in leaves and roots. Plant J. 81 (5), 781–793.

Andika, I.B., Tian, M., Bian, R., Cao, X., Luo, M., Kondo, H., Sun, L., 2023. Cros-kingdom interactions between plant and fungal viruses. Annu Rev. Virol. 119–138. https://doi.org/10.1146/annurev-virology-111821-122539.

Andika, I.B., Wei, S., Cao, C., Salaipeth, L., Kondo, H., Sun, L., 2017. Phytopathogenic fungus hosts a plant virus: a naturally occurring cross-kingdom viral infection. Proc. Natl. Acad. Sci. USA 114 (46), 12267–12272.

Aoki, S., Takebe, I., 1969. Infection of tobacco mesophyll protoplasts by tobacco mosaic virus ribonucleic acid. Virology 39 (3), 439–448.

Bian, R., Andika, I.B., Pang, T., Lian, Z., Wei, S., Niu, E., Wu, Y., Kondo, H., Liu, X., Sun, L., 2020. Facilitative and synergistic interactions between fungal and plant viruses. Proc. Natl. Acad. Sci. USA 117 (7), 3779–3788.

Boccardo, G., Lisa, V., Luisoni, E., Milne, R.G., 1987. Cryptic plant viruses. Adv. Virus. Res. 32, 171–214.

Bombarely, A., Rosli, H.G., Vrebalov, J., Moffett, P., Mueller, L.A., Martin, G.B., 2012. A draft genome sequence of *Nicotiana benthamiana* to enhance molecular plant-microbe biology research. Mol. Plant Microbe Interact. 25 (12), 1523–1530.

Brosseau, C., Moffett, P., 2015. Functional and genetic analysis identify a role for Arabidopsis ARGONAUTE5 in antiviral RNA silencing. Plant Cell 27 (6), 1742–1754.

Chen, S., 2025. fastp 1.0: an ultra-fast all-round tool for FASTQ data quality control and preprocessing. Imeta 4 (5), e70078.

Chiba, S., Lin, Y.H., Kondo, H., Kanematsu, S., Suzuki, N., 2013. Effects of defective-interfering RNA on symptom induction by, and replication of a novel partitivirus from a phytopathogenic fungus *Rosellinia necatrix*. J. Virol. 87, 2330–2341.

Chiba, S., Lin, Y.H., Kondo, H., Kanematsu, S., Suzuki, N., 2016. A novel betapartitivirus RnPV6 from *Rosellinia necatrix* tolerates host RNA silencing but is interfered by its defective RNAs. Virus. Res. 219, 62–72.

Cingolani, P., Platts, A., Wang le, L., Coon, M., Nguyen, T., Wang, L., Land, S.J., Lu, X., Ruden, D.M., 2012. A program for annotating and predicting the effects of single nucleotide polymorphisms, SnpEff: sNPs in the genome of *Drosophila melanogaster* strain w1118; iso-2; iso-3. Fly. (Austin) 6 (2), 80–92.

Coutts, R.H., Cocking, E.C., Kassanis, B., 1972. Infection of tobacco mesophyll protoplasts with tobacco mosaic virus. J. Gen. Virol. 17 (3), 289–294.

Dai, R., Yang, S., Pang, T., Tian, M., Wang, H., Zhang, D., Wu, Y., Kondo, H., Andika, I.B., Kang, Z., Sun, L., 2024. Identification of a negative-strand RNA virus with natural plant and fungal hosts. Proc. Natl. Acad. Sci. USA 121 (12), e2319582121.

Das, S., Hisano, S., Eusebio-Cope, A., Kondo, H., Suzuki, N., 2022. A transfectable fusagravirus from a Japanese strain of *Cryphonectria carpinicola* with spherical particles. Viruses 14 (8), 1722, 1710.3390/v14081722.

Di Silvestre, D., Passignani, G., Rossi, R., Ciuffo, M., Turina, M., Vigani, G., Mauri, P.L., 2022. Presence of a mitovirus is associated with alteration of the mitochondrial proteome, as revealed by protein-protein interaction (PPI) and co-expression network models in plants. Biology-Basel 11 (1), 95. https://doi.org/10.3390/biology11010095.

Esteban, R., Fujimura, T., 2003. Launching the yeast 23S RNA narnavirus shows 5′ and 3′ cis-acting signals for replication. Proc. Natl. Acad. Sci. USA 100, 2568–2573.

Esteban, R., Fujimura, T., 2021. Narnaviruses (*Narnaviridae*). In: Bamford, D., Zuckerman, M. (Eds.), Encyclopedia of Virology, 4th edn., Encyclopedia of Virology, 4th edn., 4 Elsevier, Oxford, pp. 621–626, 610.1016/B1978-1010-1012-809633-809638.820941-809632.

Fehrholz, M., Kendl, S., Prifert, C., Weissbrich, B., Lemon, K., Rennick, L., Duprex, P.W., Rima, B.K., Koning, F.A., Holmes, R.K., Malim, M.H., Schneider-Schaulies, J., 2012. The innate antiviral factor APOBEC3G targets replication of measles, mumps and respiratory syncytial viruses. J. Gen. Virol. 93 (Pt 3), 565–576.

Gamborg, O.L., Miller, R.A., Ojima, K., 1968. Nutrient requirements of suspension cultures of soybean root cells. Exp. Cell Res. 50 (1), 151–158.

Garcia-Ruiz, H., 2019. Host factors against plant viruses. Mol. Plant Pathol. 20 (11), 1588–1601.

Gelvin, S.B., 2003. *Agrobacterium*-mediated plant transformation: the biology behind the "gene-jockeying" tool. Microbiol. Mol. Biol. Rev. 67 (1), 16–37 table of contents.

Ghabrial, S.A., Caston, J.R., Jiang, D., Nibert, M.L., Suzuki, N., 2015. 50-plus years of fungal viruses. Virology. 479-480, 356–368.

Goodin, M.M., Zaitlin, D., Naidu, R.A., Lommel, S.A., 2008. *Nicotiana benthamiana*: its history and future as a model for plant-pathogen interactions. Mol. Plant Microbe Interact. 21 (8), 1015–1026.
Hillman, B.I., Cohen, A.B., 2021. Mitoviruses (*Mitoviridae*). In: Bamford, D., Zuckerman, M. (Eds.), Encyclopedia of Virology, 4th edn., Encyclopedia of Virology, 4th edn., 4 Elsevier, Oxford, p. 610. -606610.1016/B1978-1010-1012-809633-809638.821324-809631.
Jiang, Y., Liu, X., Tian, X., Zhou, J., Wang, Q., Wang, B., Yu, W., Jiang, Y., Hsiang, T., Qi, X., 2023. RNA interference of *Aspergillus flavus* in response to Aspergillus flavus partitivirus 1 infection. Front. Microbiol. 14, 1252294.
Jurvansuu, J., Kashif, M., Vaario, L., Vainio, E., Hantula, J., 2014. Partitiviruses of a fungal forest pathogen have species-specific quantities of genome segments and transcripts. Virology 462-463, 25–33.
Kim, D., Paggi, J.M., Park, C., Bennett, C., Salzberg, S.L., 2019. Graph-based genome alignment and genotyping with HISAT2 and HISAT-genotype. Nat. Biotechnol. 37 (8), 907–915.
Kim, K., Calabrese, P., Wang, S., Qin, C., Rao, Y., Feng, P., Chen, X.S., 2022. The roles of APOBEC-mediated RNA editing in SARS-CoV-2 mutations, replication and fitness. Sci. Rep. 12 (1), 14972.
Kockler, Z.W., Bostan, H., Klimczak, L.J., Hsiao, Y.C., Dennen, M.S., Cook, M.E., Mertz, T.M., Perelygina, L., Kazanov, M.D., Li, J.L., Roberts, S.A., Gordenin, D.A., 2026. APOBEC3A is the predominant global editor of cytosines in human mRNAs and in single-strand RNA viruses. G3. (Bethesda) jkag080. https://doi.org/10.1093/g1093journal/jkag1080.
Kondo, H., Sugahara, H., Fujita, M., Hyodo, K., Andika, I.B., Hisano, H., Suzuki, N., 2023. Discovery and genome characterization of a closterovirus from wheat plants with yellowing leaf symptoms in Japan. Pathogens 12 (3), 358, 310.3390/pathogens12030358.
Kotta-Loizou, I., Caston, J.R., Coutts, R.H.A., Hillman, B.I., Jiang, D., Kim, D.H., Moriyama, H., Suzuki, N., ICTV Report, C., 2020. ICTV virus taxonomy profile: *chrysoviridae*. J. Gen. Virol. 99, 19–20.
Langmead, B., Trapnell, C., Pop, M., Salzberg, S.L., 2009. Ultrafast and memory-efficient alignment of short DNA sequences to the human genome. Genome Biol. 10 (3), R25.
Li, H., Handsaker, B., Wysoker, A., Fennell, T., Ruan, J., Homer, N., Marth, G., Abecasis, G., Durbin, R., Genome Project Data Processing, S., 2009. The sequence alignment/map format and SAMtools. Bioinformatics 25 (16), 2078–2079.
Liao, Y., Smyth, G.K., Shi, W., 2014. featureCounts: an efficient general purpose program for assigning sequence reads to genomic features. Bioinformatics 30 (7), 923–930.
Lin, C.S., Hsu, C.T., Yang, L.H., Lee, L.Y., Fu, J.Y., Cheng, Q.W., Wu, F.H., Hsiao, H.C., Zhang, Y., Zhang, R., Chang, W.J., Yu, C.T., Wang, W., Liao, L.J., Gelvin, S.B., Shih, M.C., 2018. Application of protoplast technology to CRISPR/Cas9 mutagenesis: from single-cell mutation detection to mutant plant regeneration. Plant Biotechnol. J. 16 (7), 1295–1310.
Mata, C.P., Rodriguez, J.M., Suzuki, N., Caston, J.R., 2020. Structure and assembly of double-stranded RNA mycoviruses. Virus assembly and exit pathways. Adv. Virus Res. 108, 213–247.
Meinke, D.W., Cherry, J.M., Dean, C., Rounsley, S.D., Koornneef, M., 1998. *Arabidopsis thaliana*: a model plant for genome analysis. Science 282 (5389), 662–682, 662, 679-682.
Murashige, T., Skoog, F., 1962. A revised medium for rapid growth and bio sssays with tobacco tissue cultures. Physiol. Plantarum. 15 (3), 473–497.
Nagata, T., Nemoto, Y., Hasezawa, S., 1992. Tobacco BY-2 cell line as the Hela cell in the cell biology of higher plants. Int. Rev. Cytol. 132, 1–30.
Natsuaki, T., Yamashita, S., Doi, Y., Yora, K., 1979. Radish yellow edge virus, a seed-borne small spherical virus newly recognized in Japanese radish (*Raphanus sativus* L.). Ann. Phytopathol. Soc. Japan 45, 313–320.
Nerva, L., Varese, G.C., Falk, B.W., Turina, M., 2017. Mycoviruses of an endophytic fungus can replicate in plant cells: evolutionary implications. Sci. Rep. 7, 1908.
Nibert, M.L., Ghabrial, S.A., Maiss, E., Lesker, T., Vainio, E.J., Jiang, D., Suzuki, N., 2014. Taxonomic reorganization of family *Partitiviridae* and other recent progress in partitivirus research. Virus. Res. 188, 128–141.
Ohtani, M., Wachter, A., 2019. NMD-based gene regulation-A strategy for fitness enhancement in plants? Plant Cell Physiol. 60 (9), 1953–1960.
Ouibrahim, L., Caranta, C., 2013. Exploitation of natural genetic diversity to study plant-virus interactions: what can we learn from Arabidopsis thaliana? Mol. Plant Pathol. 14 (8), 844–854.
Ozkan, S., Mohorianu, I., Xu, P., Dalmay, T., Coutts, R.H.A., 2017. Profile and functional analysis of small RNAs derived from *Aspergillus fumigatus* infected with double-stranded RNA mycoviruses. BMC. Genomics. 18 (1), 416.
Pfeiffer, P., Jung, J.L., Heitzler, J., Keith, G., 1993. Unusual structure of the double-stranded RNA associated with the '447' cytoplasmic male sterility in *Vicia faba*. J. Gen. Virol. 74 (Pt 6), 1167–1173.
Quinlan, A.R., Hall, I.M., 2010. BEDTools: a flexible suite of utilities for comparing genomic features. Bioinformatics. 26 (6), 841–842.
Reed, K.M., Bargmann, B.O.R., 2021. Protoplast regeneration and its use in new plant breeding technologies. Front. Genome Ed. 3, 734951.
Roossinck, M.J., 2010. Lifestyles of plant viruses. Philos. Trans. R. Soc. Lond. B Biol. Sci. 365 (1548), 1899–1905.
Roossinck, M.J., 2019. Viruses in the phytobiome. Curr. Opin. Virol. 37, 72–76.
Sasaki, A., Kanematsu, S., Onoue, M., Oyama, Y., Yoshida, K., 2006. Infection of *Rosellinia necatrix* with purified viral particles of a member of Partitiviridae (RnPV1-W8). Arch. Virol. 151, 697–707.
Sato, Y., Hisano, S., Lopez-Herrera, C.J., Kondo, H., Suzuki, N., 2022. Three-layered complex interactions among capsidless (+)ssRNA yadokariviruses, dsRNA viruses, and a fungus. mBio 13, e0168522.
Shahi, S., Chiba, S., Kondo, H., Suzuki, N., 2021. Cryphonectria nitschkei chrysovirus 1 with unique molecular features and a very narrow host range. Virology. 554, 55–65.
Shahi, S., Hisano, S., Sa'diyah, W., Takaki, Y., Kondo, H., Suzuki, N., 2025. Thorough characterization of a new curvulavirid from a Japanese strain of *Cryphonectria nitschkei*. J. Gen. Virol. 106, 002177.
Sukegawa, S., Saika, H., Toki, S., 2021. Plant genome editing: ever more precise and wide reaching. Plant J. 106 (5), 1208–1218.
Suzuki, N., Nuss, D.L., 2002. Contribution of protein p40 to hypovirus-mediated modulation of fungal host phenotype and viral RNA accumulation. J. Virol. 76, 7747–7759.
Takebe, I., Otsuki, Y., 1969. Infection of tobacco mesophyll protoplasts by tobacco mosaic virus. Proc. Natl. Acad. Sci. USA 64 (3), 843–848.
Takenaka, M., Zehrmann, A., Verbitskiy, D., Hartel, B., Brennicke, A., 2013. RNA editing in plants and its evolution. Annu. Rev. Genet. 47, 335–352.
Telengech, P., Hisano, S., Mugambi, C., Hyodo, K., Arjona-Lopez, J.M., Lopez-Herrera, C. J., Kanematsu, S., Kondo, H., Suzuki, N., 2020. Diverse partitiviruses from the phytopathogenic fungus, *Rosellinia necatrix*. Front. Microbiol. 11, 1064, 10.10.3389/fmicb.2020.01064.
Telengech, P., Hyodo, K., Ichikawa, H., Kuwata, R., Kondo, H., Suzuki, N., 2024. Replication of single viruses across the kingdoms, fungi, Plantae, and Animalia. Proc. Natl. Acad. Sci. USA 121 (25), e2318150121.
Thorpe, T., 2012. History of plant tissue culture. Methods Mol. Biol. 877, 9–27.
Uchimiya, H., Murashige, T., 1974. Evaluation of parameters in the isolation of viable protoplasts from cultured tobacco cells. Plant Physiol. 54 (6), 936–944.
Vainio, E.J., Chiba, S., Ghabrial, S.A., Maiss, E., Roossinck, M., Sabanadzovic, S., Suzuki, N., Xie, J., Nibert, M., Ictv Report, C., 2018. ICTV virus taxonomy profile: *Partitiviridae*. J. Gen. Virol. 99 (1), 17–18.
Valvekens, D., Van Montagu, M., Van Lijsebettens, M., 1988. *Agrobacterium tumefaciens*-mediated transformation of *Arabidopsis thaliana* root explants by using kanamycin selection. Proc. Natl. Acad. Sci. USA 85 (15), 5536–5540.
Valverde, R.A., Khalifa, M.E., Okada, R., Fukuhara, T., Sabanadzovic, S., Ictv Report, C., 2019. ICTV virus taxonomy profile: *endornaviridae*. J. Gen. Virol. 100 (8), 1204–1205.
Van Norman, J.M., Benfey, P.N., 2009. *Arabidopsis thaliana* as a model organism in systems biology. Wiley. Interdiscip. Rev. Syst. Biol. Med. 1 (3), 372–379.
Velasco, L., Lopez Herrera, C.J., Cretazzo, E., 2020. Two novel partitiviruses that accumulate differentially in *Rosellinia necatrix* and *Entoleuca* sp. infecting avocado. Virus. Res. 285. https://doi.org/10.1016/j.virusres.2020.198020.
Wang, X., Kotta-Loizou, I., Coutts, R.H.A., Deng, H., Han, Z., Hong, N., Shafik, K., Wang, L., Guo, Y., Yang, M., Xu, W., Wang, G., 2024. A circular single-stranded DNA mycovirus infects plants and confers broad-spectrum fungal resistance. Mol. Plant 17 (6), 955–971.
Wilm, A., Aw, P.P., Bertrand, D., Yeo, G.H., Ong, S.H., Wong, C.H., Khor, C.C., Petric, R., Hibberd, M.L., Nagarajan, N., 2012. LoFreq: a sequence-quality aware, ultra-sensitive variant caller for uncovering cell-population heterogeneity from high-throughput sequencing datasets. Nucleic. Acids. Res. 40 (22), 11189–11201.
Wu, F.H., Hsu, C.T., Lin, C.S., 2023. Targeted insertion in *Nicotiana benthamiana* genomes via protoplast regeneration. Methods Mol. Biol. 2653, 297–315.
Yang, W., Zhai, H., Wu, F., Deng, L., Chao, Y., Meng, X., Chen, Q., Liu, C., Bie, X., Sun, C., Yu, Y., Zhang, X., Zhang, X., Chang, Z., Xue, M., Zhao, Y., Meng, X., Li, B., Zhang, X., Zhang, D., Zhao, X., Gao, C., Li, J., Li, C., 2024. Peptide REF1 is a local wound signal promoting plant regeneration. Cell 187 (12), 3024-3038 e3014.
Yue, J.J., Yuan, J.L., Wu, F.H., Yuan, Y.H., Cheng, Q.W., Hsu, C.T., Lin, C.S., 2021. Protoplasts: from isolation to CRISPR/Cas genome editing application. Front. Genome Ed. 3, 717017.